

Electronic Supplementary Information for

## **In-situ TEM observation of the structural transformation of rutile TiO<sub>2</sub> during electrochemical lithiation**

**Sung Joo Kim,<sup>a</sup> Sunyoung Noh<sup>b</sup>, Alireza Kargar<sup>b</sup>, Deli Wang<sup>b</sup>, George W. Graham<sup>a</sup>, and  
Xiaoqing Pan<sup>\*a</sup>**

<sup>1</sup> Department of Materials Science and Engineering, University of Michigan, 2300 Hayward Street, Ann Arbor, Michigan 48109, United States

<sup>2</sup>Department of Electrical and Computer Engineering, University of California-San Diego, 9500 Gilman Drive, La Jolla, California 92093, United States

## 1. Experimental

**Characterization:** High-resolution transmission electron microscopy (HR-TEM) and scanning transmission electron microscopy (HR-STEM) images of TiO<sub>2</sub> NWs were taken using JEOL JEM-3010F and aberration-corrected JEOL-JEM2100F transmission electron microscopes, operating at accelerating voltages of 300kV and 200kV, respectively.

**Assembly of the TiO<sub>2</sub> nanowire based Li-cell:** A TEM specimen was prepared by embedding NWs in Ag-based paste on a Cu post. A prepared specimen was loaded onto a single-tilt in-situ Nanofactory Instruments TEM-STM holder to be part of an electro-chemical cell assembly as an anode in a JEOL JEM-3010F microscope. Bulk Li metal, as a cathode counter-part, was scrapped onto a tungsten STM tip that was loaded on a piezo-drive of the holder inside the glove box. A naturally formed Li<sub>2</sub>O layer on the Li metal from the 3-6 sec exposure to air during transportation from an Ar-filled bag into the TEM column, acted as a solid electrolyte. The complete electro-chemical assembly was made by having the STM tip piezo-driven towards the NW. Relatively fast electro-chemical cycling, at the rate of 2V/s, was adopted in order to both restrict the quantity of Li inserted into the NW and avoid possible amorphous carbon contaminant deposition around the NW.

## 2. Supporting Figures Information

### A. Atomic structure of a rutile $\text{TiO}_2$ NW

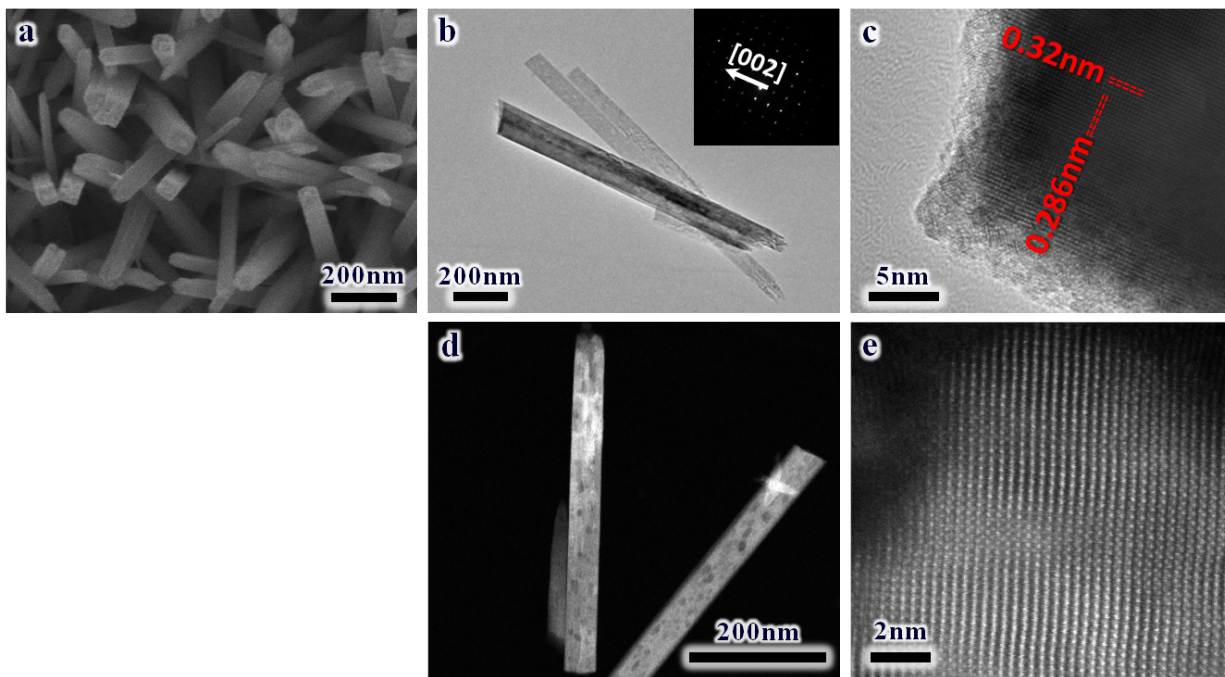


**Fig. S1.** (a) SEM image of rutile  $\text{TiO}_2$  NWs grown on a fluorine-doped tin oxide substrate. (b-e) TEM and HR-TEM images of a rutile  $\text{TiO}_2$  NW

## B. Lattice expansion of rutile $\text{TiO}_2$ upon intermediate phase transformation

Figure S2 shows lattice expansion of a rutile  $\text{TiO}_2$  NW upon intermediate phase transformation ( $\text{TiO}_2 \rightarrow \text{Li}_x\text{TiO}_2$ ) in both low- and high-magnification images. The measured lattice spacings ( $d(202)$ ) for  $\text{TiO}_2$  and  $\text{Li}_x\text{TiO}_2$  are 0.248nm and 0.250nm, respectively, the difference of which is slightly larger than that theoretically calculated. ( $d_{101}$  for  $\text{TiO}_2$  and  $\text{Li}_x\text{TiO}_2$  are 0.2487nm and 0.2489nm)

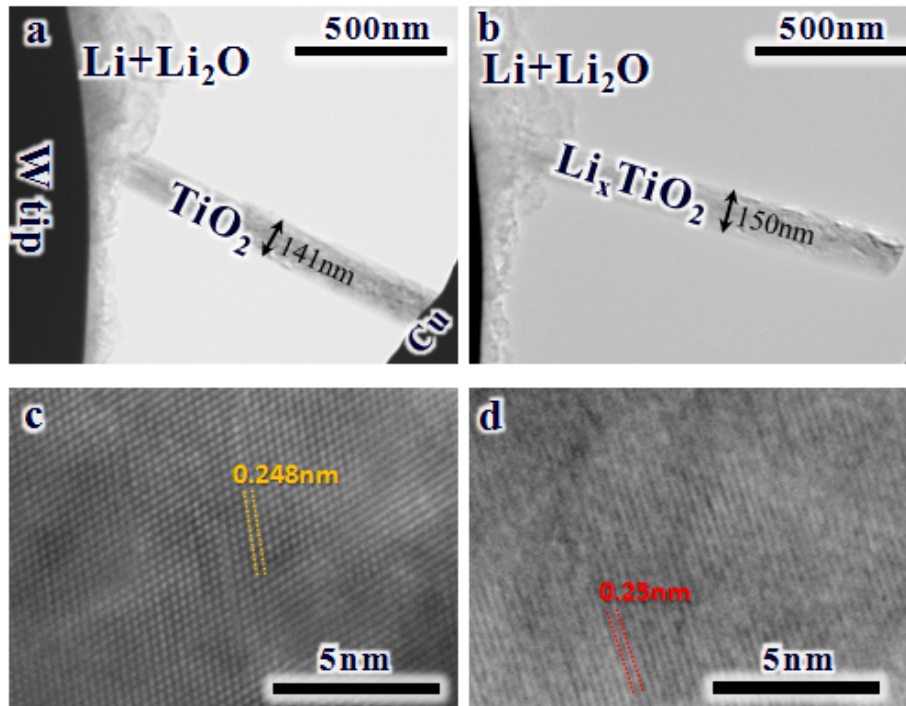


**Fig. S2** Low- and high-magnification TEM images of (a and c) a  $\text{TiO}_2$  NW in primitive state and (b and d) a  $\text{Li}_x\text{TiO}_2$  NW in transition to intermediate state.

### C. Selected area diffraction of TiO<sub>2</sub> NW before and during the phase transformation

Figure S3 shows selected area diffraction patterns of the TiO<sub>2</sub> NW (ZA: 100) before and during the phase transformation. Notice that there is a secondary diffraction pattern (yellow) overlaying the original diffraction pattern (red) (Figure S3 (b)) from the rutile phase. This agrees very well with the monoclinic phase, which marks the phase transformation from TiO<sub>2</sub> to Li<sub>x</sub>TiO<sub>2</sub>.

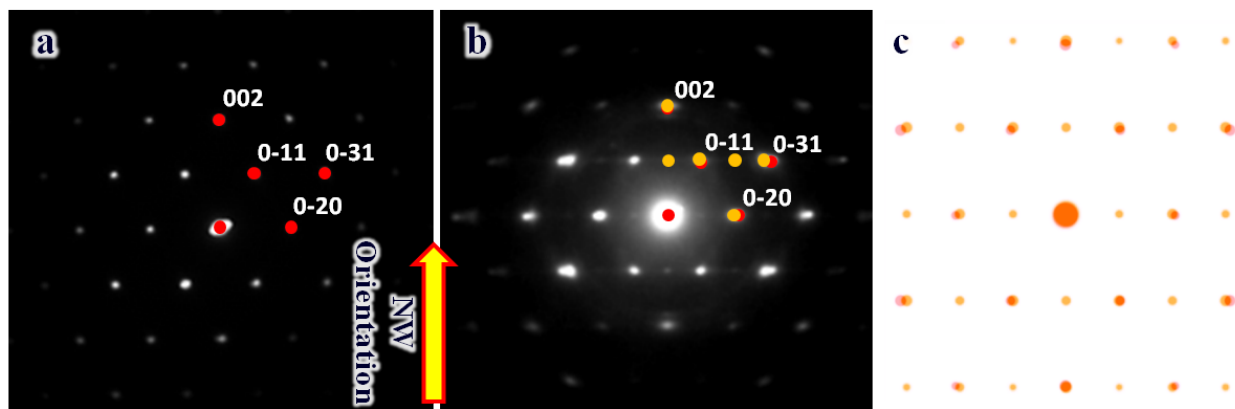


**Figure S3.** (a and b) Selected area diffraction of a primitive TiO<sub>2</sub> NW (figure S2a) and a Li<sub>x</sub>TiO<sub>2</sub> NW (figure S2b) under transition from rutile to intermediate state. Red and orange dots are the representative reciprocal spots for primitive TiO<sub>2</sub> and transformed Li<sub>x</sub>TiO<sub>2</sub>, respectively. (c) Simulated electron diffraction pattern showing phase overlap between rutile TiO<sub>2</sub> and monoclinic Li<sub>x</sub>TiO<sub>2</sub>.

#### D. Current-voltage characteristics of $\text{Li}_x\text{TiO}_2$ upon electrochemical cycling

Lithiation (during the low-resistance branch of the voltage sweep from 0 to  $-5\text{V}$ ) of the NW (e.g.,  $\text{TiO}_2 + x\text{Li}^+ + xe^- \rightarrow \text{Li}_x\text{TiO}_2$ ) induces the NW to go through the transition from a low-resistance to a high-resistance state, while the opposite is true for de-lithiation (during the high-resistance branch of the voltage sweep from 0 to  $5\text{V}$ ), as shown in Figure S4. Li-rich  $\text{Li}_x\text{TiO}_2$  exhibits Schottky-type semiconductor behavior, while Li-deficient  $\text{Li}_x\text{TiO}_2$  exhibits close-to-ohmic behavior, as reported in many literature references for other Li intercalation systems.<sup>1</sup> This transition, despite some difference in magnitude in each cycle, repeats throughout the continuous electrochemical cycling at this stage of Li intercalation.

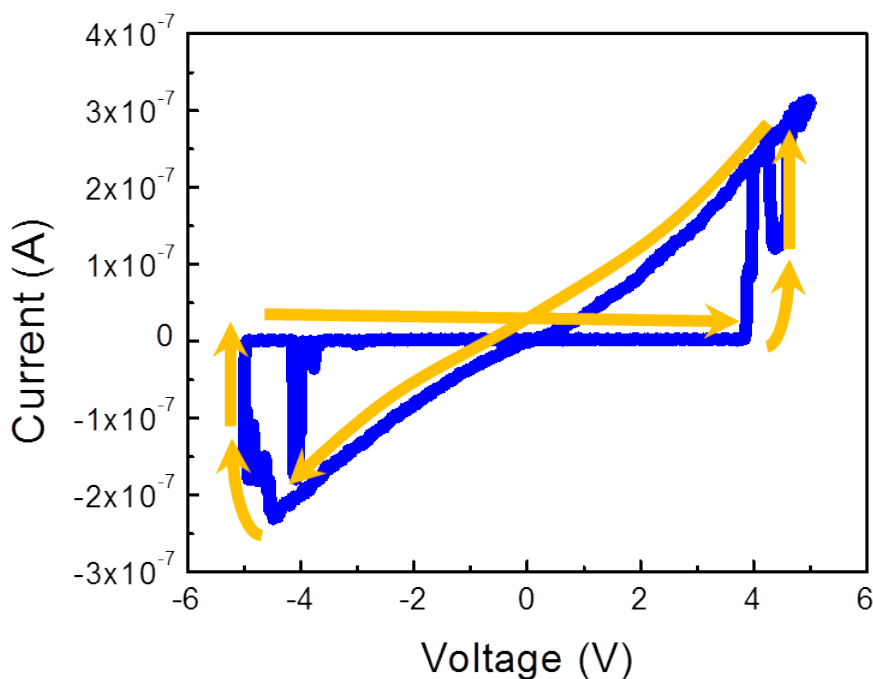


**Figure S4.** Representative graph showing the lithiation and de-lithiation behavior of the  $\text{Li}_x\text{TiO}_2$  NW under standard voltage sweep.

1 P. G. Bruce, *Chemical Communications*, 1997, 1817.

### 3. Supporting Movie Information

**Movie S1.** An in-situ TEM movie showing the fast lithiation and de-lithiation cycle of a  $\text{Li}_x\text{TiO}_2$  NW at the monoclinic phase. There is no obvious structural change observed in this intermediate regime.

**Movie S2.** An anisotropic dilation of  $\text{TiO}_2\text{-B}$  upon full lithiation at  $-4\text{V}$ , showing a bubble-like form of dilation of the  $\text{Li}_x\text{TiO}_2$  NW